Journal of Photochemistry and Photobiology A: Chemistry 200 (2008) 239–245

Contents lists available at ScienceDirect

Journal of Photochemistry and Photobiology A: Chemistry

journal homepage: www.elsevier.com/locate/jphotochem

Time-resolved EPR investigation on the photoreactions of vitamin K with antioxidant vitamins in micelle systems

Keishi Ohara*, Yoshimi Hashimoto, Chiaki Hamada, Shin-ichi Nagaoka

Department of Chemistry, Faculty of Science, Ehime University, Bunkyo-cho 2-5, Matsuyama 790-8577, Japan

ARTICLE INFO

Article history:
Received 2 May 2008
Received in revised form 23 June 2008
Accepted 24 July 2008
Available online 5 August 2008

Keywords:
Vitamin K
Vitamin C
Photolysis
EPR
Micelle

ABSTRACT

The photochemical reactions of vitamin K (VK) with antioxidant vitamins (vitamin E (VE) and vitamin C (VC)) in aqueous hexadecyltrimethylammonium chloride (CTAC), sodium dodecyl sulfate (SDS), and Triton X-100 micelle systems, and in an aerosol OT (AOT) reversed micelle system were investigated by a time-resolved EPR (TR-EPR). The photolysis of VK with VE in the aqueous micelle solutions gave the TR-EPR spectra having strong intensity and net emissive polarization, suggesting that the excited triplet state of VK ($^3VK^*$) was rapidly quenched by VE coexisting inside the micelle. On the other hand, the photolysis of VK with VC in the aqueous SDS and CTAC micelle systems gave the spectra having weak intensity, showing that the reaction between $^3VK^*$ and VC was inefficient in these micelle systems, probably because $^3VK^*$ scarcely diffused out from the micelle. The photolysis of VK with VC in the AOT reversed micelle solution gave the spin-correlated radical pair CIDEP spectrum. The result suggests that the long-lived radical pair was generated from the reaction between $^3VK^*$ and VC in the water/oil interface region of the AOT micelle, although one of the reactants dissolved in the oil phase and another did in the separated water phase.

1. Introduction

In biological systems, many compounds are working as antioxidants for protecting living bodies from oxidative stresses [1–5]. Vitamin E (VE) and vitamin C (VC) are typical and well-known naturally available antioxidants. Several studies have been performed for the antioxidant actions of VE and VC [1–11]. The natural VEs, such as α, β, γ, and δ-tocopherols, have a long alkyl-chain and are oily compounds. They are localized in the hydrophobic region of biological membranes, and protect membranes from lipid peroxidation [1–5]. The inhibition of the peroxidation is partly ascribed to the hydrogen atom transfer (HAT) from the phenolic hydroxyl group of a tocopherol (TocH) to LOO• and the production of the corresponding tocopheroxyl radical (Toc•, Reaction (1)) [1–3,6], where LOO• and LOOH stand for a lipid peroxyl radical and the corresponding hydroperoxide, respectively. However, the subsequent reduction of Toc• is necessary for the effective antioxidation because Toc• itself often induces lipid peroxidation. VC (Fig. 1) is a water-soluble antioxidant contained in vegetables, fruits, and leaves of teas, and also existing in human blood. VC is believed to reduce Toc• and regenerate TocH in the water–oil (w/o) interface region of biomembranes (Reaction (2)) [7–11]:

$$LOO^\bullet + TocH \rightarrow LOOH + Toc^\bullet \quad (1)$$

$$Toc^\bullet + VC \rightarrow TocH + VC \quad (2)$$

Biological quinones, for example ubiquionones and vitamin Ks (VKs), are widely distributed in biological systems and play important roles as redox carriers of various proteins and enzymes in processes, such as photosynthesis, oxidative phosphorylation, and mitochondrial electron transport [12–17]. VKs are 1,4-napthoquinone (NQ) derivatives, and play important roles in the photoelectron transport system in photosynthetic reaction center, therefore, vitamin K_1 (phylloquinone, Fig. 1) is distributed in chloroplast on leaves of green plants, and vitamin K_2 (menaquinone) is in rhodobacteria [12–15]. VKs are also well known to be required for normal blood clotting in animals and human beings. Ubiquinone, generally known as coenzyme-Q (CoQ), is a 1,4-benzoquinone derivative distributed in mitochondrial membranes, lysosomes, and Golgi vesicles [16,17]. Because ubiquinol (the reduced form of ubiquinone) is a superior lipid-soluble antioxidant, CoQ is recently used widely in supplements, skin-care products, and cosmetics for the purpose of the damage-care and anti-aging health. These biological quinones are, however, effective photo-initiators of lipid peroxidation, and the excited-state quinones produced by UV light irradiation can directly and indirectly damage membranes, peptides, and DNAs. Furthermore,

* Corresponding author. Tel.: +81 89 927 9596; fax: +81 89 927 9590.
E-mail address: ohara@chem.sci.ehime-u.ac.jp (K. Ohara).

1010-6030/$ – see front matter © 2008 Elsevier B.V. All rights reserved.
doi:10.1016/j.jphotochem.2008.07.011

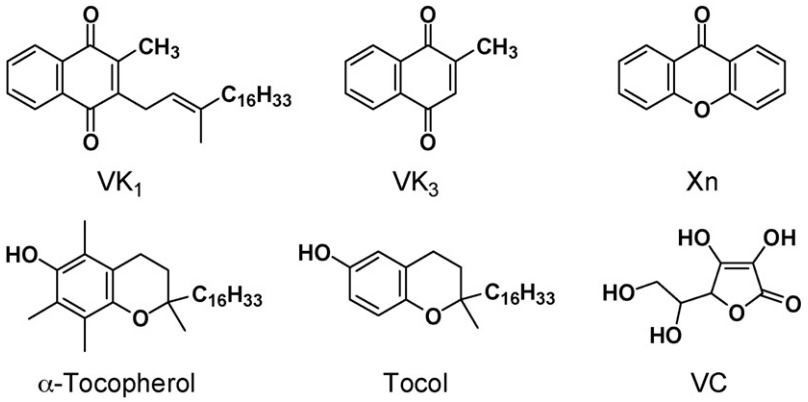

Fig. 1. Molecular structures of vitamin K_1 (VK_1), K_3 (VK_3), xanthone (Xn), α-tocopherol, tocol, and ascorbic acid (VC).

the excited triplet states of quinones are known to be efficient sensitizers of singlet oxygen production [18,19]. Because photo-degradations are actually induced in photo-irradiated tissues, such as skins of animals and leaves of plants, photo-initiated injuries to biological systems and the protection mechanisms against them have been of great interest for several decades [20–23].

In the present study, the photo-induced reactions of VK with antioxidant vitamins (VE and VC) in various micelle systems were investigated by using a time-resolved EPR (TR-EPR) technique. The photo-induced reactions of VK with antioxidants in inhomogeneous media having w/o phases are thought to be models for biological protection processes versus photo-degradations around membranes. In such systems, lipid-soluble VK and VE should exist in the hydrophobic region, whereas VC should in the water-rich region. Therefore, the reaction between the excited VK and VC is expected to occur at the w/o interface region. TR-EPR is a suitable tool for investigating photo-induced reactions, not only because it can detect and identify short-lived intermediate radicals directly, but also because it can observe the chemically induced dynamic electron polarization (CIDEP) phenomena [24–27]. CIDEP spectra often provide information on the reaction mechanism and on the interaction between intermediate radicals within microseconds after photoexcitation. The information related to biological protection mechanisms versus photo-initiated injuries is expected to obtain from the TR-EPR results on the kinetics and the interaction between intermediate radicals at the w/o interface region of micelles.

2. Experimental

Vitamin K_1 (VK_1), K_3 (menadione, 2-methyl-1,4-napthoquinone, VK_3, Fig. 1), and VC (ascorbic acid, AsH_2, Fig. 1) were commercially available special grade reagents (Wako Pure Chemicals) and were used without further purification. Tocol (Fig. 1) was prepared according to the reported method [28], and was used as a VE model for simplification of the EPR spectrum. *n*-Hexane, isooctane (2,2,4-trimethylpentane), and 2-propanol were commercially available special grade reagents (Wako) and were used as received. Hexadecyltrimethylammonium chloride (CTAC), sodium dodecyl sulfate (SDS), Triton X-100 (TX-100), and aerosol OT (AOT, sodium bis(2-ethyl-1-hexyl)sulfosuccinate) were commercially available reagents (Nacalai Tesque) and were used as received. Deionized water was treated by an ion-exchange column (Millipore Milli-Q). The concentration of each surfactant (SDS, CTAC, and TX-100) in the aqueous micelle solution was kept at 5.0 wt.%. The concentration of AOT in the reversed micelle solution was kept at 1.0×10^{-1} mol dm^{-3} (M). The ratio of water and isooctane (w/o value) of the AOT system was always kept at 1/100 (v/v).

TR-EPR measurements were carried out at room temperature by using a X-band EPR spectrometer (JEOL JES-FE2XG or FA-100) without field modulation [29,30]. A Nd-YAG laser (Continuum Surelight-I, THG 355 nm, 9.7 Hz) was used for photoexcitation. TR-EPR spectra at several delay times were recorded by a boxcar integrator (Stanford Research System SR-250) whose gate width

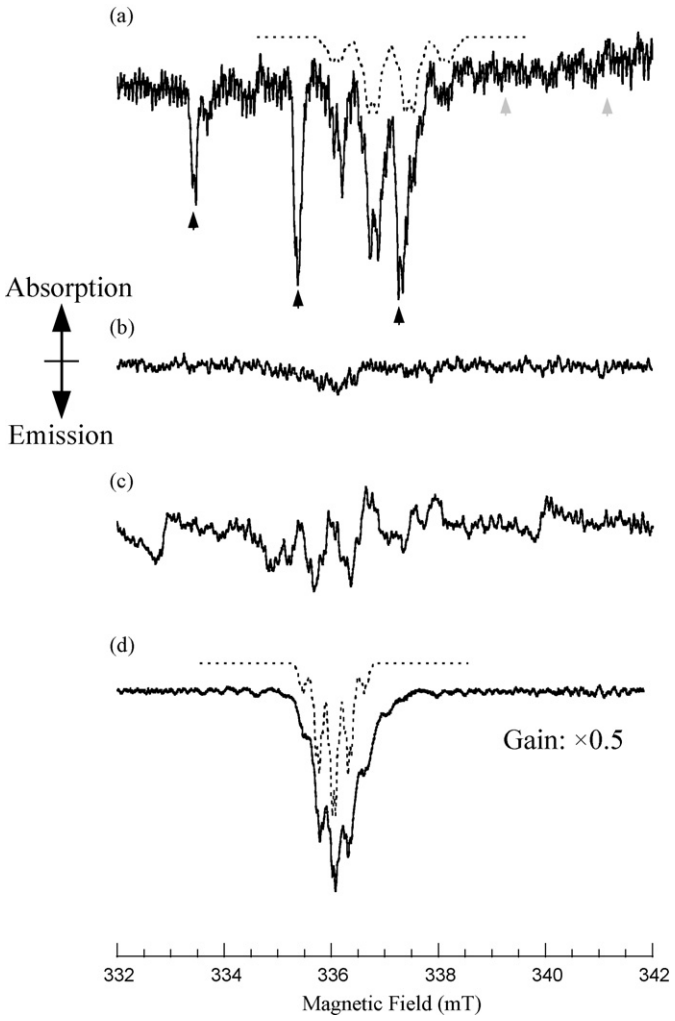

Fig. 2. CIDEP spectra observed at the delay time of 1.2 μs on the photolysis of VK_3 in (a) 2-propanol, (b) CTAC micelle, (c) SDS micelle, and (d) TX-100 micelle solutions. Broken lines show the simulated spectra of (a) $VK_3H^{\bullet}$ and (d) $VK_3^{\bullet -}$ using parameters given in the text.

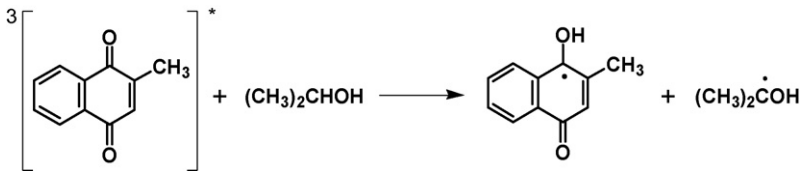

Scheme 1.

was kept at 0.2 μs. The sample solutions were deoxygenated by bubbling with N_2 gas before and during experiments, and flowed through a quartz flat cell (optical path 0.3 mm) in the EPR cavity.

3. Results and discussion

3.1. The photoreactions of VK_3 in 2-propanol and in the aqueous micelle systems

The CIDEP spectrum observed on the photolysis of VK_3 (1.0×10^{-3} M) in 2-propanol at the delay time of 1.2 μs after the photoexcitation is shown in Fig. 2a. The EPR spectrum was assigned to a superposition of the semiquinone radical of VK_3 ($VK_3H^{\bullet}$; $g = 2.0043$, A_H(3 equivalent protons) = 0.684 mT, $A_H(1) = 0.059$ mT, and $A_{OH} = 0.155$ mT) [31,32] and the 2-hydroxypropan-2-yl radical ($2HP^{\bullet}$; $g = 2.0031$, $A_H(6) = 1.97$ mT, and $A_{OH} = 0.055$ mT) [29]. The hyperfine coupling constants (HFCs) of $VK_3H^{\bullet}$ were estimated by the spectral simulation according to the spin densities calculated by the Hückel–McLauchlan method. The broken line shown in Fig. 2a is the simulated spectrum of $VK_3H^{\bullet}$ according to the above HFC values, and the black and gray arrows indicate the EPR lines of $2\text{-}HP^{\bullet}$. These radicals were produced by a hydrogen abstraction of the excited triplet state of VK_3 ($^3VK_3^*$) from solvent 2-propanol [32]. The spectrum showing total emission with a slight *E*/*A* (low field side emission/high field side absorption) distortion can be explained by a superposition of the dominant net emissive polarization due to the triplet mechanism (TM) and a small *E*/*A* polarization due to the ST_0 mixing (ST_0M) radical pair mechanism (RPM) [24–27]. The dominant TM contribution indicates that $^3VK_3^*$ reacted with solvent 2-propanol faster than the spin-lattice relaxation in $^3VK_3^*$ (Scheme 1). This result is similar to that reported for NQ [31].

The CIDEP spectra observed at the delay time of 1.2 μs on the photolysis of VK_3 (5.0×10^{-4} M) in the aqueous CTAC, SDS, and TX-100 micelle solutions are shown in Fig. 2b, c, and d, respectively. VK_3 is a little soluble in water, but in the micelle solutions most of VK_3 molecules should exist inside the micelle. The EPR spectrum in the CTAC micelle system (Fig. 2b) was broadened, very weak, and *E*/*A* polarized, suggesting that the radical generating reaction was slow and a minor process here. In the SDS micelle system (Fig. 2c), the *E*/*A* antiphase lines were observed in the CIDEP spectrum, which indicated the formation of the spin-correlated radical pair (SCRP) between $VK_3H^{\bullet}$ and the SDS-origin alkyl radical trapped together inside the micelle [33]. This fact is consistent with the observation of the magnetic field effect (MFE) reported in this system [34,35], because MFE is enhanced by the restriction of free diffusion of radicals. On the other hand, in the TX-100 micelle system (Fig. 2d), the CIDEP spectrum showed large intensity and total emission, suggesting that $^3VK_3^*$ reacted with TX-100 fast enough to conserve large amount of the TM polarization. In the TX-100 system, the EPR spectrum spreading over smaller magnetic field area than the $VK_3H^{\bullet}$ spectrum in Fig. 2a is thought to come from the anion-type radical of VK_3 ($VK_3^{\bullet-}$). The broken line shown in Fig. 2d is the simulated spectrum of $VK_3^{\bullet-}$ ($g = 2.0044$, $A_H(3) = 0.301$ mT, $A_H(1) = 0.238$ mT, and $A_H(4) = 0.064$ mT) according to the reported HFC values [36,37]. $VK_3^{\bullet-}$ is thought to be generated by the dissociation of a proton from $VK_3H^{\bullet}$ in the aqueous media. The formation of the anion radical in the TX-100 micelle was also reported for NQ [31,37,38]. In other words, $^3VK_3^*$ inside the micelle reacted with the surfactant molecules in SDS and TX-100 micelle systems, and scarcely reacted in the CTAC micelle system.

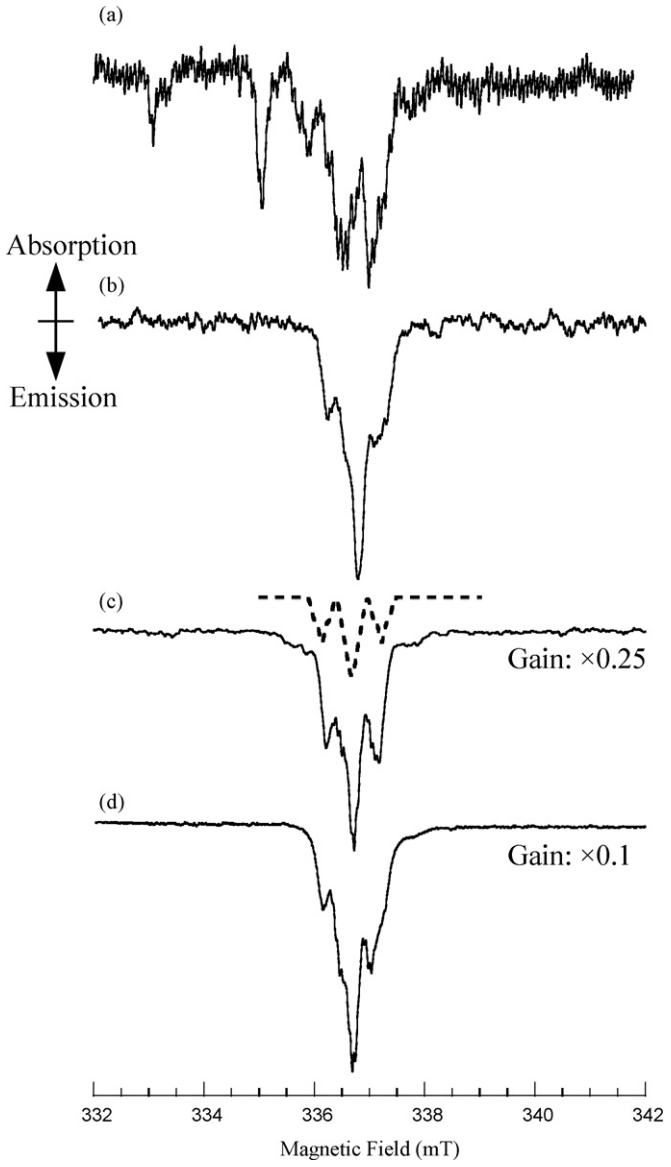

Fig. 3. CIDEP spectra observed at the delay time of 1.2 μs on the photolysis of VK_3 with tocol in (a) 2-propanol, (b) CTAC micelle, (c) SDS micelle, and (d) TX-100 micelle solutions. Broken line shows the simulated spectrum of $Toc^{\bullet}$ using parameters given in the text.

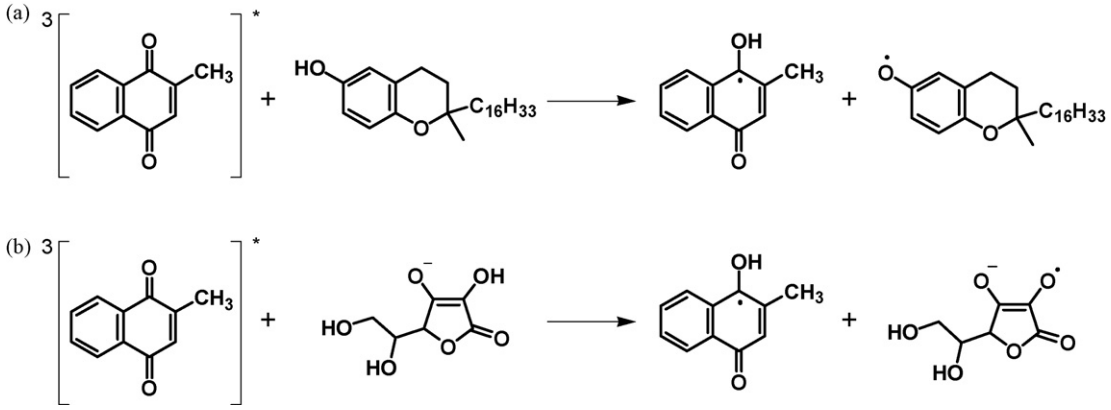

Scheme 2.

3.2. The photoreactions of VK_3 with tocol in 2-propanol and in the aqueous micelle systems

The CIDEP spectrum observed at the delay time of 1.2 μs on the photolysis of VK_3 (1.0×10^{-3} M) with tocol (1.0×10^{-2} M) in 2-propanol is shown in Fig. 3a. The spectrum resembles Fig. 2a, but is somewhat broadened. It is explained by a superposition of the tocopheroxyl radical in addition to $VK_3H^{\bullet}$ and $2HP^{\bullet}$. These radicals were produced by the hydrogen abstraction of $^3VK_3^*$ from 2-propanol and tocol. The spectrum showing total emission with a slight *E*/*A* distortion can be explained by the TM and ST_0M-RPM contributions. $^3VK_3^*$ reacted fast with tocol (Scheme 2a) as well as solvent 2-propanol in this homogeneous solution.

The CIDEP spectra observed at the delay time of 1.2 μs on the photolysis of VK_3 (5.0×10^{-4} M) in the aqueous CTAC, SDS, and TX-100 micelle solutions are shown in Fig. 3b, c, and d, respectively. In these micelle systems, both VK_3 and tocol should exist inside the micelle. The spectra obtained in these micelle systems resemble each other. From the spectral simulation, the spectra in CTAC (Fig. 3b) and TX-100 (Fig. 3d) are explained by a superposition of those of the tocopheroxyl radical ($g = 2.0047$, $A_H(1) = 0.578$ mT, $A_H(1) = 0.508$ mT, $A_H(1) = 0.052$ mT, and $A_H(2) = 0.132$ mT) [39] and $VK_3^{\bullet -}$, while that in SDS (Fig. 3c) is explained by a superposition of those of the tocopheroxyl radical and $VK_3H^{\bullet}$. The reason for generating the $VK_3H^{\bullet}$ in the SDS micelle system might be that the negative charge of the SDS micelle surface inhibited the anion radical formation. The strong signal intensity and the total emission polarization of the spectra indicate that $^3VK_3^*$ reacted with tocol coexisting inside the micelle fast enough to conserve large amount of the TM polarization (Scheme 2a).

3.3. The photoreactions of VK_3 with VC in 2-propanol/H_2O and in the aqueous micelle systems

The CIDEP spectrum observed at the delay time of 1.2 μs on the photolysis of VK_3 (1.0×10^{-3} M) with VC (1.0×10^{-2} M) in the mixed solvent (2-propanol/H_2O = 9/1, v/v) is shown in Fig. 4a. The spectrum resembles Figs. 2a and 3a. It is explained by a superposition of the ascorbate monoanion radical ($As^{\bullet -}$) as a pair of EPR lines ($g = 2.0054$ and $A_H(1) = 0.19$ mT) [30] in addition to $VK_3H^{\bullet}$ and $2HP^{\bullet}$. $VK_3H^{\bullet}$, $2HP^{\bullet}$, and $As^{\bullet -}$ were produced by the hydrogen abstraction of $^3VK_3^*$ from 2-propanol and VC. The total emission CIDEP with a slight *E*/*A* distortion is explained in terms of a superposition of a dominant net emissive component due to TM and a small contribution of ST_0M-RPM. $^3VK_3^*$ reacted with VC (Scheme 2b) as well as solvent 2-propanol.

The CIDEP spectra observed at the delay time of 1.2 μs on the photolysis of VK_3 (5.0×10^{-4} M) with VC (1.0×10^{-2} M) in the aqueous CTAC, SDS, and TX-100 micelle solutions are shown in Fig. 4b, c, and d, respectively. Almost similar results were obtained by using sodium ascorbate in place of AsH_2. In these systems, water-soluble VC should be dissolved in the bulk water phase outside the micelle,

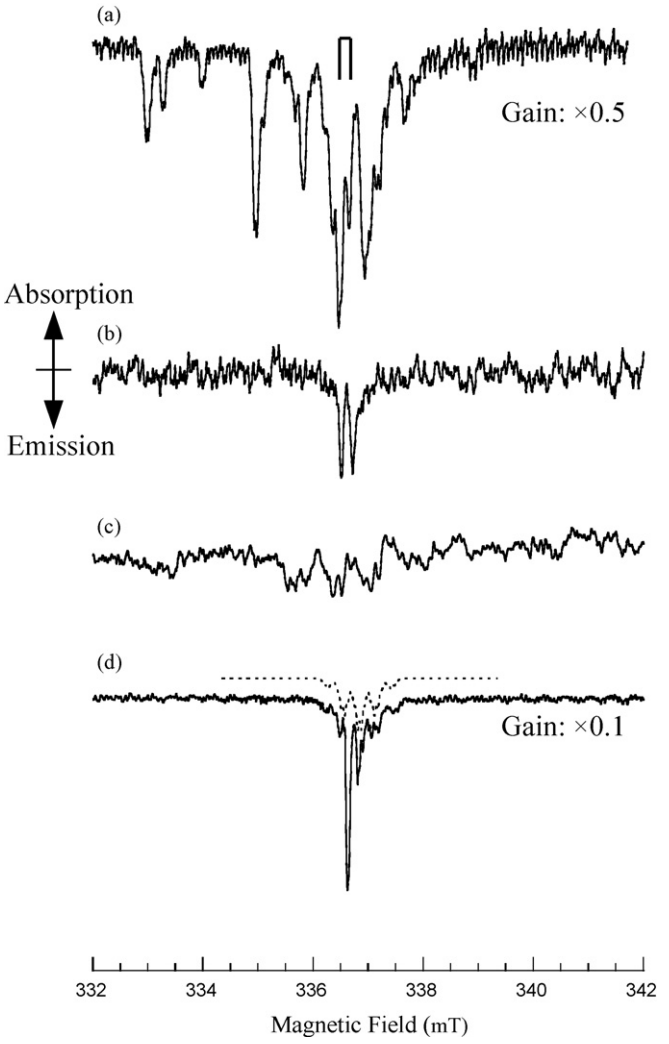

Fig. 4. CIDEP spectra observed at the delay time of 1.2 μs on the photolysis of VK_3 with VC in (a) the mixed solvent (2-propanol/H_2O = 9/1, v/v), (b) CTAC micelle, (c) SDS micelle, and (d) TX-100 micelle solutions. Stick diagram shows the EPR lines of $As^{\bullet -}$. Broken line shows the simulated spectra of $VK_3^{\bullet -}$ using parameters given in the text.

while VK_3 should exist inside the micelle. Thus, the reaction of $^3VK_3^*$ with VC is expected to occur in the w/o interface region of the micelle. The EPR lines due to $As^{\bullet-}$ was observed in the CTAC micelle system (Fig. 4b), and a little contribution of the VK_3-origin radical might be overlapped. The result suggests that $^3VK_3^*$ partly reacted with VC. Most of VC should exist as the monoanion form (AsH^-) because VC releases a proton in aqueous solutions according to the acid–base equilibrium ($pK_{a1} = 4.16$) [30]. AsH^- should be attracted to the CTAC micelle surface having positive charge, and may partly adsorb on the micelle surface. Thus, $^3VK_3^*$could react with VC on the surface of the CTAC micelle. Previously, the TR-EPR investigation on the photoreaction of xanthone (Xn) with VC in the aqueous micelle systems was reported [30]. In the Xn case, the strong signal of $As^{\bullet-}$ coming from the fast reaction of the excited triplet state of Xn ($^3Xn^*$) with VC was observed in the CTAC micelle system. The signal intensity obtained for the present VK_3 system was rather smaller than that for the Xn system. It indicates that the photoreaction of VK_3 with VC in the CTAC micelle system is inefficient compared with that of Xn. The diffusion of $^3VK_3^*$ from inside to surface of the micelle may be limited for some reasons.

In the SDS micelle system (Fig. 4c), the *E*/*A* antiphase lines were observed similar to Fig. 2c, also indicating the formation of the SCRP between $VK_3H^\bullet$ and the SDS-origin radical. The result indicates that $^3VK_3^*$ did not react with VC but reacted with the SDS molecule. The negative charge of the SDS micelle surface keeps AsH^- away from the micelle by the charge repulsion force. Thus, the reaction of $^3VK_3^*$ with VC needs the exit of $^3VK_3^*$ from the micelle. In the reported Xn case, even in the SDS micelle system, small amount of $^3Xn^*$ could react slowly ($\sim 10^7\ s^{-1}$) with VC because $^3Xn^*$ could exit from the micelle with the rate constant of $1.7 \times 10^6\ s^{-1}$ [30,40]. The photoreaction of lipid-soluble Xn with water-soluble VC was controlled by the displacement dynamics of $^3Xn^*$ from the micelle. The present VK_3 photoreaction can be interpreted similarly. The lack of $As^{\bullet-}$ in the spectrum indicates that $^3VK_3^*$ could scarcely exit from the SDS micelle.

On the other hand, the EPR signal intensity obtained in the TX-100 micelle system (Fig. 4d) was very strong, suggesting the fast reaction of $^3VK_3^*$. The pair of sharp EPR lines due to the $As^{\bullet-}$ shows E^*/A polarization explained by a superposition of TM and ST_0M-RPM. The relatively weak peaks around the EPR lines of $As^{\bullet-}$ was assigned to $VK_3^{\bullet-}$. The broken line shown in Fig. 4d is the simulated spectrum of $VK_3^{\bullet-}$ [36,37]. The $VK_3^{\bullet-}$ spectrum shows almost symmetrical total emission polarization, while that of $As^{\bullet-}$ shows the E^*/A distortion. The result suggests that the formation processes of $VK_3^{\bullet-}$ and $As^{\bullet-}$ were not completely the same as each other. $^3VK_3^*$ can react with both the TX-100 molecule and VC. The large contribution of the total emission due to TM in $VK_3^{\bullet-}$, suggesting the fast reaction, may come from the large contribution of the reaction between $^3VK_3^*$ and TX-100 occurring inside the micelle. The E^*/A polarization due to TM and RPM observed in $As^{\bullet-}$ suggests that the reaction between $^3VK_3^*$ and VC was slightly slower than that with TX-100. In the reported Xn case, the strong and symmetric total emission polarization was observed for both the Xn radical and $As^{\bullet-}$ in the TX-100 system, indicating that the fast reaction occurred between $^3Xn^*$ and VC [30]. It was explained that small amount of VC was included in the relatively polar region of the TX-100 micelle and reacted with $^3Xn^*$ inside the micelle. The present VK_3 case can be considered similarly. The TR-EPR result for VK_3 may suggest that the $^3VK_3^*$ was included in more hydrophobic area or that the diffusion of $^3VK_3^*$ to the polar area of the TX-100 micelle including VC was somewhat restricted.

In the aqueous micelle systems, the reaction of $^3VK_3^*$ inside the micelle with VC outside the micelle was rather limited compared with that of $^3Xn^*$. It is explained that $^3VK_3^*$ can scarcely exit from the micelle within its lifetime. $^3VK_3^*$ may be trapped strongly in the hydrophobic area of the micelle, otherwise the lifetime of $^3VK_3^*$ might be shortened by the fast reaction with the surfactants.

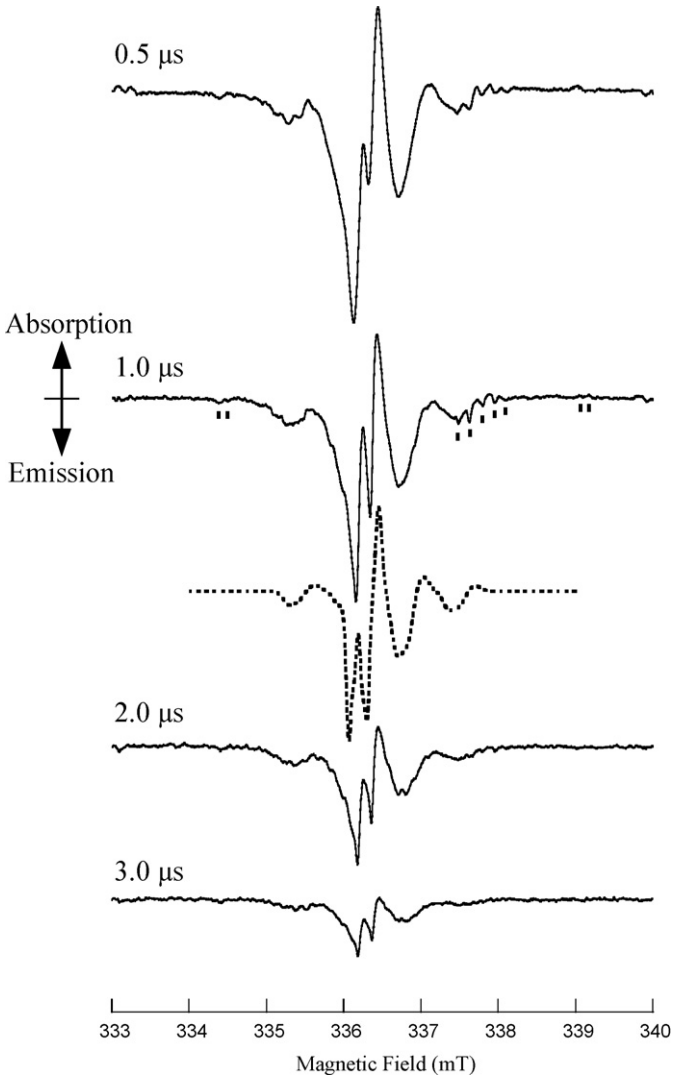

Fig. 5. Time evolution of CIDEP spectrum observed on the photolysis of VK_3 with VC in the AOT reversed micelle solution.

3.4. The photoreactions of VKs with VC in the reversed AOT micelle systems

The AOT reversed micelle system, as generally known, consists of a water pool inside the micelle and a hydrophobic bulk phase outside the micelle. In the AOT reversed micelle system, water-soluble VC should exist inside the micelle, while VK_3 should be dissolved in the bulk phase outside the micelle. Thus, the photoreaction of VK_3 with VC is expected to occur around the w/o interface region of the reversed micelle. The time evolution of the CIDEP spectrum observed on the photolysis of VK_3 (5.0×10^{-4} M) with VC (1.0×10^{-2} M) in the AOT (0.10 M) reversed micelle system in isooctane (w/o = 1/100) is shown in Fig. 5. Almost similar results were obtained in the AOT micelle system by using *n*-hexane in place of isooctane. The specific *E*/*A* antiphase lines in the center of the spectrum clearly indicate the formation of the SCRP [33,41–43]. The strong antiphase lines around the center come from $As^{\bullet-}$ and the broad bands spreading over 4 mT come from $VK_3H^\bullet$. Thus, the SCRP should consist of $As^{\bullet-}$ and $VK_3H^\bullet$, which were produced by the hydrogen abstraction reaction of $^3VK_3^*$ from VC (Scheme 2b). The

weak and sharp satellite lines marked by dots in Fig. 5 are due to the AOT-origin alkyl-type radical generated by the sub-reactions [44]. The steady-state EPR measurement on this system with the 10 Hz laser excitation gave the spectrum of $As^{\bullet-}$ as two triplet hyperfine lines ($g = 2.0054$, $A_H(1) = 0.199$ mT, and $A_H(2) = 0.020$ mT). The simulated SCRP spectrum by using the value $J = -0.10$ mT for the exchange integral of the SCRP and the HFCs of $As^{\bullet-}$ and $VK_3H^{\bullet}$ described above is shown as a broken line in Fig. 5. Although the detail description for the SCRP kinetics was discussed in several reports [45–48], here we used the simple classical SCRP CIDEP model for the simulation [41–43]. The simulated spectrum is in good agreement with the observed one. The time evolution of the spectrum observed in 0.5–3.0 μs shows the SCRP spectrum decayed keeping its shape. It indicates that the strong interaction in the SCRP was kept more than 3 μs, suggesting that both radicals were trapped and their free diffusions were inhibited. The increase of w/o (1/50) in the AOT system gave the decrease of the $|J|$ value in the SCRP spectrum, suggesting that the size of the water pool inside the reversed micelle influenced the inter-radical dynamics in the SCRP. These results indicate that neutral $VK_3H^{\bullet}$ was trapped near the water pool of the AOT micelle.

VK_3 was dissolved in bulk oil phase. However, $^3VK_3^*$ generated near the micelle can diffuse to the w/o interface region of the reversed micelle, probably because $^3VK_3^*$ has larger polarity than VK_3. The reaction of $^3VK_3^*$ with VC occurred rapidly in the w/o interface region, and the produced radicals interacted with each other and formed the SCRP. The long-lived SCRP indicates that the $VK_3H^{\bullet}$ did not diffuse away from the w/o interface region, probably because $VK_3H^{\bullet}$ has large polarity enough to be trapped there.

The time evolution of the CIDEP spectrum observed on the photolysis of VK_1 (5.0×10^{-3} M) with AsH_2 (1.0×10^{-3} M) in the AOT (0.10 M) reversed micelle system in isooctane (w/o = 1/100) is shown in Fig. 6. VK_1 is more hydrophobic than VK_3 because it has an additional long alkyl-chain. A pair of sharp EPR lines observed in the center of spectrum at the delay time of 1.0 and 2.0 μs is due to $As^{\bullet-}$ and the broad peaks overlapped with them should be due to the VK_1 semiquinone radical ($VK_1H^{\bullet}$) [32]. The weak signal intensity in the VK_1 system might come from the fact that the reaction of the triplet state of VK_1 ($^3VK_1^*$) with VC was inefficient compared with that of VK_3. The photoexcited VK_1 is known to cause the intramolecular reaction and to generate the quinone methide [15,32]. The total emission with a slight *E*/*A* distortion polarization in the spectrum is explained in terms of a superposition of the TM contribution and the additional ST_0M-RPM contribution. In the spectra at the delay time of 1.0 and 2.0 μs, each EPR line of $As^{\bullet-}$ shows the *E*/*A* antiphase line shape, indicating the SCRP contribution clearly. However, the exchange interaction in the SCRP was estimated to be rather smaller ($|J| \sim 0.05$ mT) than that for the above VK_3 system. It may come from the hydrophobic property of VK_1 having a long alkyl-chain. The inter-radical distance between $VK_1H^{\bullet}$ and $As^{\bullet-}$ may be larger than that between $VK_3H^{\bullet}$ and $As^{\bullet-}$, because the long alkyl-chain of $VK_1H^{\bullet}$ pulls itself into the bulk hydrophobic phase. The rise of $As^{\bullet-}$ for the VK_1 system seems to be slower than that for the VK_3 system. The fact may suggest that the reaction between $^3VK_1^*$ and VC occurred slower than that between $^3VK_3^*$ and VC. The reason for this can be explained by the following way. The reaction of $^3VK_1^*$ with VC should occur in the w/o interface region. Therefore, the diffusion of $^3VK_1^*$ to the w/o interface region was required, however, it was delayed by the long alkyl-chain of VK_1 pulling into the bulk hydrophobic phase. The $As^{\bullet-}$ lines decayed in 3 μs, suggesting that the radical quenching or diffusion occurred in a few microseconds. The evidence of the SCRP component was not observed clearly in the broad spectrum of $VK_1H^{\bullet}$ having emissive polarization. The $VK_1H^{\bullet}$ spectrum remained for more than 3.0 μs keeping its shape. The emissive polarization of $VK_1H^{\bullet}$ may partially come from processes other than the reaction between $^3VK_1^*$ and VC. $^3VK_1^*$ in the bulk phase might react with the solvent and AOT. Otherwise, the emissive polarization due to the radical-triplet pair mechanism might be induced in $VK_1H^{\bullet}$ through the interaction between $VK_1H^{\bullet}$ and $^3VK_1^*$ in the bulk phase [49,50].

The present CIDEP results in the AOT reversed micelle system demonstrate the clear evidence of the spontaneous formation of SCRP in the w/o interface region around the micelle surface. The excited lipid-soluble molecules, such as $^3VK_3^*$ and $^3VK_1^*$, in the hydrophobic bulk phase outside the reversed micelle, diffuse to the w/o interface region and react rapidly with the water-soluble antioxidant VC in the water pool inside the reversed micelle (Fig. 7). The VK radicals have larger polarity than their parent molecules and might be trapped in the polar region around the water pool, as a result, the SCRP can form with $As^{\bullet-}$. In particular, the SCRP generated between $VK_3H^{\bullet}$ and $As^{\bullet-}$ showed the strong and long-lived interaction. It might be explained that the polarity of $VK_3H^{\bullet}$ is large enough to be trapped in the polar environment around the reversed micelle. The VK_1 system also showed the formation of SCRP, whose interaction was, however, rather smaller than that in the VK_3

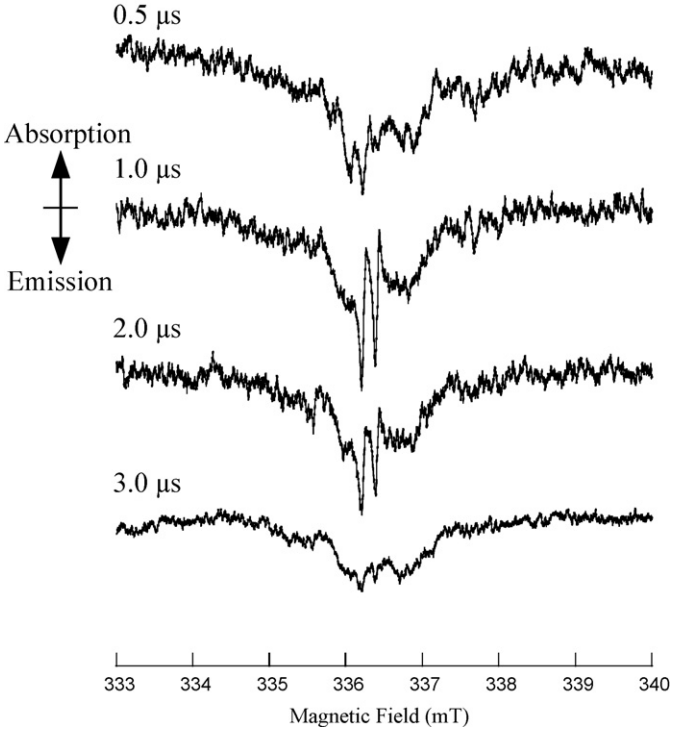

Fig. 6. Time evolution of CIDEP spectrum observed on the photolysis of VK_1 with VC in the AOT reversed micelle solution.

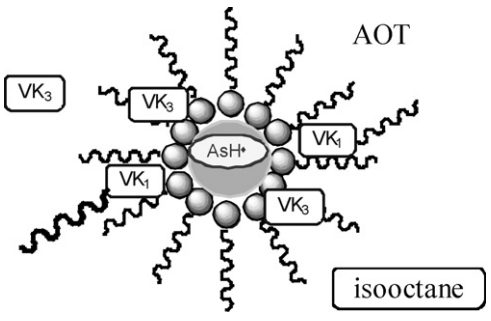

Fig. 7. Schematic diagram of the photoreaction of VK with VC in the AOT reversed micelle system.

system. The long-lived SCRP has usually been observed in the restricted system, such as alkyl-chain linked molecules and reactants dissolving together inside the micelle. In fact, the SCRP in the AOT reversed micelle system was reported for 9,10-anthraquinone-1,5-disulfonate (AQS) [51,52]. In the AQS system, however, since AQS is water-soluble, the generated SCRP was restricted in the water pool inside the reversed micelle. The present VK_3 system might be a rare case showing the long-lived SCRP although one of the reactants dissolved in the oil phase and another did in the separated water phase. The observation of the long-lived SCRP predicts the large MFE in the present AOT reversed micelle systems. On the other hand, no SCRP signal for $As^{\bullet -}$ was observed in aqueous micelle systems because $As^{\bullet -}$ diffused in the bulk water phase.

4. Conclusions

In the present study, the photoreactions of VK with VE and VC in the various micelle systems were investigated by TR-EPR. The photolysis of VK with VE in the aqueous micelle solutions gave the TR-EPR spectra having strong intensity and net emissive polarization, suggesting that $^3VK^*$ was rapidly quenched by VE coexisting inside the micelle. On the other hand, the photolysis of VK with VC in the aqueous SDS and CTAC micelle systems gave the spectra having weak intensity, showing that the reaction between $^3VK^*$ and VC was inefficient in these systems, probably because $^3VK^*$ scarcely diffused out from the micelle. The photolysis of VK with VC in the AOT reversed micelle system gave the SCRP CIDEP spectrum, suggesting that the reaction between $^3VK^*$ and VC occurred rapidly in the w/o interface region and produced the long-lived radical pair, although one of the reactants dissolved in the oil phase and another did in the water phase. The present results suggest that both VE and VC can work as the antioxidants versus the photo-initiated injuries induced by the excited quinones in biological systems. In particular, the antioxidant reaction of VC versus the excited quinones would be strongly controlled by the transportation of the reactants to the w/o interface region of biomembranes.

Acknowledgments

This work was supported by Grant-in-Aid for Scientific Research C (16550016 and 19550019) from the Japan Society for the Promotion of Science (JSPS). K.O. is grateful to Prof. Emeritus K. Mukai for his supports.

References

[1] M. Mino, H. Nakamura, A.T. Diplock, H.J. Kayden (Eds.), Vitamin E, Japan Scientific Society Press, Tokyo, 1993.
[2] G.W. Burton, K.U. Ingold, Acc. Chem. Res. 19 (1986) 194–201.
[3] E. Niki, Chem. Phys. Lipids 44 (1987) 227–253.
[4] K. Fukuzawa, W. Ikebata, A. Shibata, I. Kumadaki, T. Sakanaka, S. Urano, Chem. Phys. Lipids 63 (1992) 69–75.
[5] K. Fukuzawa, Y. Inokami, A. Tokumura, J. Terao, A. Suzuki, BioFactors 7 (1998) 31–40.
[6] S. Nagaoka, A. Kuranaka, H. Tsuboi, U. Nagashima, K. Mukai, J. Phys. Chem. 96 (1992) 2754–2761.
[7] J.E. Packer, T.F. Slater, R.L. Willson, Nature 278 (1979) 737–738.
[8] E. Niki, T. Saito, A. Kawakami, Y. Kamiya, J. Biol. Chem. 259 (1984) 4177–4182.
[9] K. Mukai, M. Nishimura, S. Kikuchi, J. Biol. Chem. 266 (1991) 274–278.
[10] R.H. Bisby, A.W. Parker, Arch. Biochem. Biophys. 317 (1995) 170–178.
[11] A. Watanabe, N. Noguchi, M. Takahashi, E. Niki, Chem. Lett. (1999) 613–614.
[12] L. Stryer, Biochemistry, Freeman, New York, 1975.
[13] C.M. Jackson, Y. Nemerson, Annu. Rev. Biochem. 49 (1980) 765–811.
[14] I. Sieckmann, A. van der Est, H. Bottin, P. Sétif, D. Stehlik, FEBS Lett. 284 (1991) 98–102.
[15] M.-A. Hangarter, A. Hörmann, Y. Kamdzhilov, J. Wirz, Photochem. Photobiol. Sci. 2 (2003) 524–535.
[16] M. Bentinger, K. Brismar, G. Dallner, Mitochondrion 7S (2007) S41–S50.
[17] V.E. Kagan, P.J. Quinn (Eds.), Coenzyme Q: Molecular Mechanisms in Health and Disease, CRC Press LLC, Boca Raton, FL, 2001.
[18] A.P. Darmanyan, C.S. Foote, J. Phys. Chem. 97 (1993) 5032–5035.
[19] Z.D. Markovic, K.L. Patterson, Photochem. Photobiol. 58 (1993) 329–334.
[20] S.Y. Wang (Ed.), Photochemistry and Photobiology of Nucleic Acid, Academic Press, New York, 1976, pp. 1–2.
[21] H.F. Blum, Photodynamic Action and Diseases Caused by Light, Hafner, New York, 1964.
[22] R.B. Webb, Photochem. Photobiol. Rev. 2 (1977) 169.
[23] J. Jagger, Photochem. Photobiol. 18 (1973) 353–354.
[24] S. Nagakura, H. Hayashi, T. Azumi (Eds.), Dynamic Spin Chemistry, Kodansha, Tokyo, 1998 (Chapter 7).
[25] H. van Willigen, P.R. Levstein, M.H. Ebersole, Chem. Rev. 93 (1993) 173–197.
[26] K.A. McLauchlan, J.H. Hore, in: A.J. Hoff (Ed.), Advanced EPR: Application in Biology and Biochemistry, Elsevier, Amsterdam, 1989.
[27] H. Murai, J. Photochem. Photobiol. C 3 (2003) 183–201.
[28] J.L.G. Nilsson, H. Sievertsson, H. Selander, Acta Chem. Scand. 22 (1968) 3160.
[29] K. Ohara, K. Mukai, Chem. Phys. Lett. 317 (2000) 619–623.
[30] K. Ohara, R. Watanabe, Y. Mizuta, S. Nagaoka, K. Mukai, J. Phys. Chem. B 107 (2003) 11527–11533.
[31] Y. Nishioku, K. Ohara, K. Mukai, S. Nagaoka, J. Phys. Chem. B 105 (2001) 5032–5038.
[32] M.T. Craw, C. Depew, J.K.S. Wan, J. Magn. Reson. 65 (1985) 339–343.
[33] G.L. Closs, M.D.E. Forbes, J.R. Norris, J. Phys. Chem. 91 (1987) 3592–3599.
[34] Y. Sakaguchi, H. Hayashi, J. Phys. Chem. 88 (1984) 1437–1440.
[35] Y. Gao, J. Chen, Y. Pan, X. Zhuang, S. Yu, Colloids Surf. A 287 (2006) 126–131.
[36] M.R. Das, H.D. Connor, D.S. Leniart, J.H. Freed, J. Am. Chem. Soc. 92 (1970) 2258–2268.
[37] T.-X. Lu, G.-Z. Li, X.-Z. Li, W.-B. Sun, Q. Wu, Acta Chim. Sin. 56 (1998) 1046–1047.
[38] G.-Z. Li, J.-H. Mu, X.-Z. Li, L.-M. Zhai, T.-X. Lu, G.-L. Dai, Colloids Surf. A 194 (2001) 263–270.
[39] K. Mukai, N. Tsuzuki, S. Ouchi, K. Fukuzawa, Chem. Phys. Lipids 30 (1982) 337–345.
[40] N. Mohtat, F.L. Cozens, J.C. Scaiano, J. Phys. Chem. B 102 (1998) 7557–7562.
[41] C.D. Buckley, D.A. Hunter, P.J. Hore, K.A. McLauchlan, Chem. Phys. Lett. 135 (1987) 307–312.
[42] K. Maeda, M. Terazima, T. Azumi, Y. Tanimoto, J. Phys. Chem. 95 (1991) 197–204.
[43] R. Bittl, S.G. Zech, Biochim. Biophys. Acta 1507 (2001) 194–211.
[44] R.C. White, V. Gorelik, E.G. Bagryanskaya, M.D.E. Forbes, Langmuir 23 (2007) 4183–4191.
[45] E. Bagryanskaya, M. Fedin, M.D.E. Forbes, J. Phys. Chem. A 109 (2005) 5064–5069.
[46] V.F. Tarasov, H. Yashiro, K. Maeda, T. Azumi, I.A. Shkrob, Chem. Phys. 226 (1998) 253–269.
[47] V.F. Tarasov, H. Yashiro, K. Maeda, T. Azumi, I.A. Shkrob, Chem. Phys. 212 (1996) 353–361.
[48] A.A. Neufeld, P.A. Purtov, A.B. Doktorov, Chem. Phys. Lett. 273 (1997) 311–320.
[49] A. Kawai, K. Shibuya, J. Photochem. Photobiol. C 7 (2006) 89–103.
[50] K. Ohara, N. Hirota, Bull. Chem. Soc. Jpn. 69 (1996) 1517–1526.
[51] N.J. Turro, I.V. Khudyakov, J. Phys. Chem. 99 (1995) 7654–7662.
[52] K. Akiyama, S. Tero-Kubota, J. Phys. Chem. B 106 (2002) 2398–2403.